



## ON INTERACTION BETWEEN MODE III CRACK AND A NONIDEAL BIMATERIAL INTERFACE

G. S. M I S H U R I S (RZESZÓW)

Behaviour of a stress field in a neighbourhood of a crack tip placed near a nonideal interface is investigated. Along the interface tractions are continuous, but displacements are assumed to be discontinuous, and proportional to the tractions. Coefficient of proportionality depends on a geometrical form of the interfacial zone.

### INTRODUCTION

Local effects around a crack tip and the nearest bimaterial interface play an important role in fracture mechanics of composites [3, 5]. Because structures of modern composites are very complicated, we cannot directly solve the corresponding boundary value problems. For this purpose, the Finite Element Method may be applied. In such an approach, special elements should be used, and sizes of regions in which these elements are taken into account should be estimated. Theoretical works by Zak, Williams, Cherepanov, Sih, Rice, Erdogan, Comninou, Atkinson, Hutchinson and many others have made it possible to establish the main regularities of the interaction between a crack tip and a bimaterial interface. However, such interface has usually been considered as an “ideal” contact, when the vectors of the displacements and tractions were continuous across the interface. The objective of this work is to discuss local stress and strain states, accounting for mechanical features of “nonideal” contact. Two different situations are separately investigated. In the first part of the paper we assume that the crack tip terminates at the nonideal interface, but in the second one, the crack tip is situated at some distance from the interface.

#### 1. STRESS SINGULARITY NEAR CRACK TIP TERMINATING AT THE INTERFACE

We shall investigate such a mathematical model that, firstly, must be as simple as possible to solve the arising boundary value problems, and, secondly, must preserve the main regularities of the mechanical feature of the interface.

Namely, we consider the Mode III (antiplane) problem for a semi-infinite crack, terminating normally at the interface of a bimaterial plane. We assume that there is a thin adhesive elastic zone between the materials (of the shear moduli  $\mu_0$  and  $\mu_1$ ). Thickness of the interfacial zone satisfies the relation  $h(r) = Ar^\alpha$ , where  $r$  is the distance from the crack tip to an arbitrary point on the interface. Further on we propose that  $OY$ -axis coincides with the crack line ahead, but the origin of the coordinate is at the crack tip. Considering such interlayers as thin elastic shells, we can find interactive conditions along the interface:

$$(1) \quad [\sigma_{\theta z}]|_{\theta=0} = 0, \quad ([u] - \tau r^\alpha \sigma_{\theta z})|_{\theta=0} = 0.$$

For this purpose, we integrate a respective balance equation in a curvilinear coordinate with respect to a parameter determining the direction which is perpendicular to the shell boundaries. Here parameter  $\tau$  is calculated as follows:  $\tau = A/\mu_{\text{int}} \ll 1$ , where  $\mu_{\text{int}}$  is the shear modulus of the elastic interlayer. Because the geometry of the problem does not contain two parameters with dimension of length, we normalize all distances by the characteristic length where tractions act along the crack surfaces.

Such an approach makes it possible to investigate different geometry of the intermediate zone depending on the values of the parameters  $\tau$  and  $\alpha$ . So, if  $\tau = 0$  we have the usual ideal contact conditions. When  $\tau > 0$ , nonideal contact arises. Namely, if  $\alpha = 0$  then there is a thin layer between the materials. The situation when  $0 < \alpha < 1$  can be interpreted as a thin adhesive zone with damage near the crack tip. For  $\alpha = 1$ , the intermediate zone is constructed by two thin wedges. Finally,  $1 < \alpha$  can represent an "almost ideal" contact between the materials.

### 1.1. Problem formulation

We will find the harmonic function  $u = u_z$  satisfying the intermediate conditions (1) across the interface. Along the crack surfaces the traction is prescribed:

$$(2) \quad \sigma_{\theta z}|_{\theta=-\pi/2} = -g(r),$$

but on the crack line ahead one can conclude due to symmetry that

$$(3) \quad u|_{\theta=\pi/2} = 0.$$

Finally, we should assume additional conditions in the singular points ( $r \rightarrow 0$ ,  $r \rightarrow \infty$ ) of the domain under consideration.

$$(4) \quad u(r, \theta) = \begin{cases} O(r^{\vartheta_0}), & r \rightarrow 0, \\ O(r^{-\vartheta_\infty}), & r \rightarrow \infty, \end{cases} \quad \sigma(r, \theta) = \begin{cases} O(r^{\gamma_0-1}), & r \rightarrow 0, \\ O(r^{-\gamma_\infty-1}), & r \rightarrow \infty. \end{cases}$$

Here  $\vartheta_0, \vartheta_\infty \geq 0$ ,  $(\vartheta_0 + \vartheta_\infty) > 0$ ,  $\gamma_0, \gamma_\infty > 0$  are some unknown constants which depend on the values of  $\mu_0, \mu_1, \tau, \alpha$  and will be calculated by solving the problem.

### 1.2. Reduction of the problem to a functional equation

Applying the Mellin transform technique we obtain the following functional equation

$$(5) \quad \mu_0 \tau \tilde{\sigma}_0(s + \alpha - 1) + F(s) \tilde{\sigma}_0(s) = G(s),$$

against the function

$$(6) \quad \tilde{\sigma}_0(s) = \int_0^{\infty} \sigma_{\theta z}(r, \theta)|_{\theta=0} r^s dr,$$

which is analytic in view of (4) in the strip  $-\gamma_0 < \operatorname{Re} s < \gamma_{\infty}$ . Here we introduce the notations:

$$F(s) = \frac{2(\kappa - \cos \pi s)}{(1 - \kappa)s \sin \pi s}, \quad G(s) = \frac{\tilde{g}(s)}{s \sin(\pi s/2)},$$

$$\tilde{g}(s) = \int_0^{\infty} g(r) r^s dr, \quad \kappa = \frac{\mu_0 - \mu_1}{\mu_0 + \mu_1}.$$

Besides, to ensure the balance of the domain  $-\pi/2 < \theta < 0$  we should assume that

$$(7) \quad \tilde{\sigma}_0(0) = -\tilde{g}(0).$$

In the case of ideal contact ( $\tau = 0$ ), Eq. (5) is directly solved in a closed form, of course. This solution is well known (see for example [3]). Particularly, one can conclude that  $\vartheta_0 = \vartheta_{\infty} = \gamma_0 = \gamma_{\infty} = \omega$ , where  $\omega \in (0, 1)$  is the first zero of the function  $F(s)$  which is nearest to the imaginary axis.

Equation (5) is also immediately solved in the case of nonideal contact across the thin wedges ( $\alpha = 1$ ) for an arbitrary value of  $\tau$ . Then,  $\vartheta_0 = \vartheta_{\infty} = \gamma_0 = \gamma_{\infty} = \omega_*(\tau)$ , where  $\omega_*(\tau)$  is the mentioned first zero of the function  $F_{\tau}(s) = \mu_0 \tau + F(s)$ . The corresponding graph is presented in Fig. 1. Let us note that the normalized parameter  $\tau_0 = \tau \mu_0$  is not small, in general. This fact is in a contradiction to the situation where parameter  $\tau \ll 1$ . Besides, the additional condition (7) holds automatically true for these two cases.

In the general case of the nonideal contact ( $\tau > 0$ ,  $\alpha \neq 1$ ), Eq. (5) is reduced to a special singular integral equation on a half-axis with fixed point singularities. Such equations have been investigated in [8]. We shall not present here the procedure of reduction of that equation, or analyse the obtained singular equation (for this purpose see Appendices in [9, 10]).

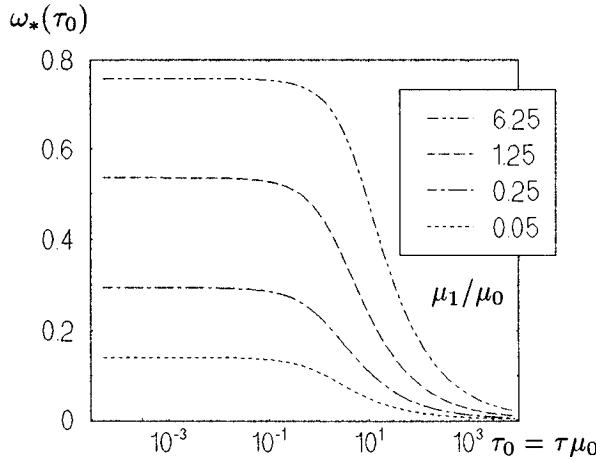


FIG. 1. Graph of the parameter  $\omega_*(\tau_0)$  determining the exponent of stress singularity  $\gamma_0 - 1 = \omega_*(\tau_0) - 1$  for the case  $\alpha = 1$ .

1.3. Asymptotics of the solution near singular points

Let us remember that in the case of the ideal contact conditions, a solution near zero and infinity points can be estimated as follows:

$$(8) \quad \begin{aligned} u(r, \theta) &= O(r^\omega), & \sigma_{r(\theta)z}(r, \theta) &= O(r^{\omega-1}), & r &\rightarrow 0, \\ u(r, \theta) &= O(r^{-\omega}), & \sigma_{r(\theta)z}(r, \theta) &= O(r^{-1-\omega}), & r &\rightarrow \infty. \end{aligned}$$

Accurate relations are presented in [3]. What is important to note is that there are no other singular terms in these asymptotic relations.

For the nonideal contact, the situation changes depending on the values of the parameters  $\alpha, \tau$ . Namely, when the adhesive zone is a thin layer ( $\alpha = 0, \tau > 0$ ), asymptotic expansion of solution of the problem is of the form

$$(9) \quad \begin{aligned} u^{(0)}(r, \theta) &= C_0 - \frac{C_0}{\tau_0} r \sin \theta + O(r^{1+\omega}), & r &\rightarrow 0, \\ u^{(1)}(r, \theta) &= -\frac{C_0 \mu_0 r}{\pi \mu_1 \tau_0} [(\pi - 2\theta) \sin \theta + 2(C_1 + \ln r) \cos \theta] + O(r^{1+\omega}), & r &\rightarrow 0, \\ \sigma_{r(\theta)z}^{(0)}(r, \theta) &= g_{r(\theta)}^{(0)}(\theta) + O(r^\omega), & r &\rightarrow 0, \\ \sigma_{r(\theta)z}^{(1)}(r, \theta) &= g_{r(\theta)}^{(1)}(\theta) + g_{r(\theta)}^{(2)}(\theta) \ln r + O(r^\omega), & r &\rightarrow 0, \\ u^{(j)}(r, \theta) &= O(r^{-\omega}), & \sigma_{r(\theta)z}^{(j)}(r, \theta) &= O(r^{-1-\omega}), & r &\rightarrow \infty, \end{aligned}$$

where  $C_0, C_1$  are some constants, and superscript  $j$  ( $j = 0, 1$ ) indicates in which materials (with the shear moduli  $\mu_0$  or  $\mu_1$ , respectively) the relations are true.

These formulae can be obtained from [9] by taking into account the symmetry of the problem under consideration. Moreover, forms of the functions  $g_{r(\theta)}^{(j)}$  are easily found from strain-stress relations.

For all remaining cases ( $\tau > 0$ ,  $\alpha > 0$ ), the corresponding relations can be rewritten like this:

$$\begin{aligned}
 u^{(0)}(r, \theta) &= C_0 + \frac{k_3}{\mu_0 \gamma_0} r^{\gamma_0} \operatorname{ctg}(\gamma_0 \pi / 2) \cos \gamma_0(\pi / 2 + \theta) + O(r^{\gamma_0^*}), \quad r \rightarrow 0, \\
 u^{(1)}(r, \theta) &= \frac{k_3}{\mu_1 \gamma_0} r^{\gamma_0} \sin \gamma_0(\pi / 2 - \theta) + O(r^{\gamma_0^*}), \quad r \rightarrow 0, \\
 (10) \quad \sigma_{r(\theta)z}^{(j)}(r, \theta) &= k_3 r^{\gamma_0 - 1} g_{r(\theta)}^{(j)}(\theta, \gamma_0) + O(r^{\gamma_0^* - 1}), \quad r \rightarrow 0, \\
 u^{(0)}(r, \theta) &= C_\infty + O(r^{-\gamma_\infty}), \quad u^{(1)}(r, \theta) = O(r^{-\gamma_\infty}), \quad r \rightarrow \infty, \\
 \sigma_{r(\theta)z}^{(j)}(r, \theta) &= O(r^{-1 - \gamma_\infty}), \quad r \rightarrow \infty.
 \end{aligned}$$

Here, the constant  $k_3$  in the principal term of stress asymptotics is the so-called "Generalized Stress Intensity Factor", which coincides with SIF when  $\gamma_0 = 0.5$ . Taking into account this fact, further on we shall call it SIF. Let us here note that situations can arise that several singular terms ( $\gamma_0^* < 1$ ) of stress asymptotics appear near the crack tip, what is in contradiction to the case of the ideal interface.

These relations have been derived in [10]. Let us discuss the results obtained in [10] for exponents of the singular terms of stress field near the crack tip:

- For  $\alpha = 0$ , stress concentration appears only in front of the crack tip for any values of the mechanical parameters  $\mu_0, \mu_1, \tau$ , and it has a logarithmic character. Passing to the displacement field, there is a displacement discontinuity along the bimaterial interfacial contact near the crack tip ( $C_0 \neq 0$ ), and other parameters in Eq. (4) are  $\vartheta_0 = 0, \vartheta_\infty = \omega$ .

- If  $\alpha \in (0, 0.5]$ , only one singular term in asymptotic expansion of stress in the neighbourhood of the crack tip appears. The corresponding exponent is  $\gamma_0 - 1 = -\alpha \in (-1, 0)$ , and it is independent of  $\mu_0, \mu_1, \tau$ .

- For the case  $\alpha \in (0.5, 1)$ , or more precisely  $\alpha \in (\alpha_n^-, \alpha_{n+1}^-)$ , ( $n = 2, 3, \dots$ ), where  $\alpha_n^- = 1 - 1/n$ , there are exactly  $n$  singular terms in the asymptotics with the exponents  $\gamma_0 - 1 = -\alpha, \gamma_j^- - 1 = (j + 1)(1 - \alpha) - 1 \in (-1, 0), j = 1, \dots, n$ . Constants in these terms can be calculated from some recurrent relations (see [10]). In the last two cases ( $\alpha \in (0, 1)$ ), the displacement discontinuity along the bimaterial interface near the crack tip also appears ( $C_0 \neq 0$ ), and  $\vartheta_0 = 0, \vartheta_\infty = \omega$ .

- If  $\alpha = 1$ , there is one singular term of stress asymptotics with the exponent  $\omega_* - 1 \in (-1, \omega - 1)$ , depending essentially on the values of the mechanical

parameters  $\mu_0, \mu_1, \tau$  (see Fig. 1). For example, when  $\tau \rightarrow 0$  we have  $\omega_* - 1 \rightarrow \omega - 1$ . This coincides with the result for the ideal contact. In this case ( $\alpha = 1$ ) and the next one ( $\alpha > 1$ ), the displacement field is continuous near the crack tip ( $C_0 = 0$ ). However, it is discontinuous at any distance from the crack tip along the bimaterial contact in view of the conditions (1). Besides,  $\vartheta_0 = \gamma_0$ .

- For the case  $\alpha \in (1, 2 - \omega)$ , or more precisely  $\alpha \in (\alpha_{n+1}^+, \alpha_n^+)$ , ( $n = 2, \dots$ ), where  $\alpha_n^+ = 1 + (1 - \omega)/(n - 1)$ , there are exactly  $n$  singular terms in the asymptotic expansion of stresses with the exponents  $\gamma_0 - 1 = \omega - 1$ ,  $\gamma_j^+ - 1 = -j(\alpha - 1) + \omega - 1 \in (-1, 0)$ ,  $j = 1, \dots, n$ .

- Finally, in the case  $\alpha \in [2 - \omega, \infty)$ , one singular term in the asymptotic expression for stress appears. The corresponding exponent is of the form  $\gamma_0 - 1 = \omega - 1$ , and does not depend on the remaining parameters. Thus, the formula of the solution is of the same form as for the ideal interface (8).

What is interesting to note is that there are two cases (where  $\alpha = 1/2$  and  $\mu_1/\mu_0 = 1$ ; or  $\alpha = 1 + \omega$ ) when the corresponding constants  $k_3$  in the main terms of expressions (10) can be calculated in a closed form.

Passing to the behaviour of the solution in the neighbourhood of the infinite point ( $r \rightarrow \infty$ ), we only note that

$$\begin{aligned} 0 \leq \alpha < 1: & \quad C_0 \neq 0, \quad C_\infty = 0, & \quad \gamma_0 = 1 - \alpha, \quad \gamma_\infty = \omega, \\ \alpha = 1: & \quad C_0 = 0, \quad C_\infty = 0, & \quad \gamma_\infty(\tau_0) = \gamma_0(\tau_0) = \omega_*(\tau_0), \\ 1 < \alpha < \infty: & \quad C_0 = 0, \quad C_\infty \neq 0, & \quad \gamma_0 = \omega - 1, \quad \gamma_\infty = \alpha - 1. \end{aligned}$$

#### 1.4. Numerical results and discussion

Now we present some numerical results concerning the stress intensity factors for loading in (2)  $g(r) = \delta(r - 1)$  (the Dirac delta-function concentrated at the unit distance from the crack tip on the crack surface), and for different values of the remaining mechanical parameters of the problem:  $\mu_1/\mu_0, \alpha, \tau_0$ . Here it is more convenient for us to use a dimensionless parameter  $\tau_0 = \tau\mu_0$  instead of  $\tau$ . Further on, we shall separately consider two cases  $\alpha \in (0, 0.5]$  and  $\alpha \in [2, \infty)$ , since they have their specific features (there is always only one singular term in the asymptotic expansion of stress field near the crack tip).

First of all, we investigate the influence of the normalized parameter  $\tau_0 = \tau\mu_0$  on the coefficients in (10).

Thus, in the case of  $\alpha = 0.1$  in Fig. 2 graphs of the stress intensity factor  $k_3$  (Fig. 2 a) and the normalized jump of displacement near crack tip  $C_0\mu_0$  (Fig. 2 b) (see (10)) are presented in a logarithmic scale, as functions of  $\tau_0$  for different values of the ratio  $\mu_1/\mu_0$ . As it can be easily seen, the corresponding curves are

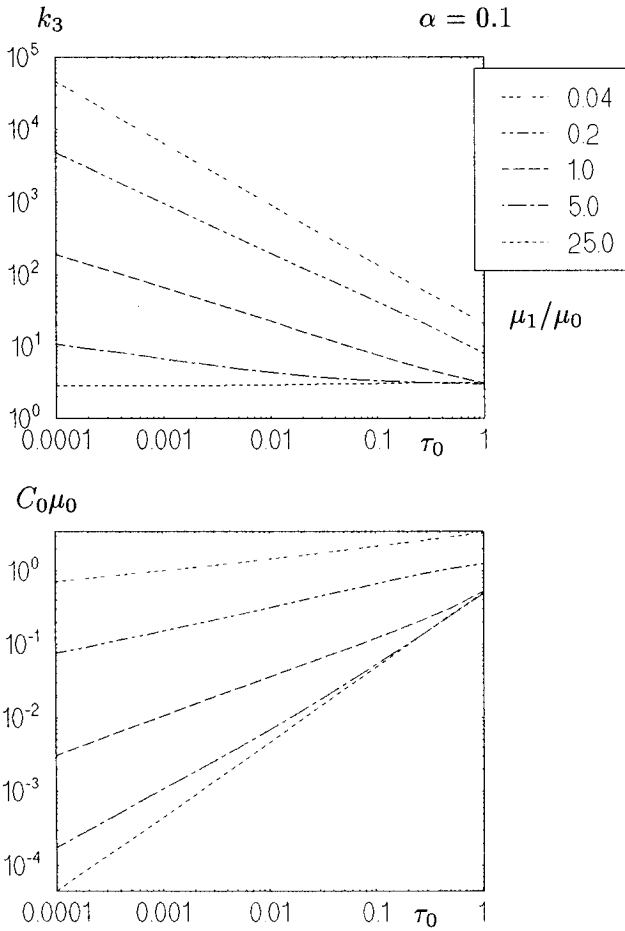


FIG. 2. Graphs of the generalized SIF  $k_3$  and displacement discontinuity near the crack tip  $C_0\mu_0$  for different values of  $\tau_0 = \mu_0\tau$ .

straight lines for all values of parameter  $\tau_0$  under consideration. Consequently, we can conclude that

$$(11) \quad C_0 \sim \tau_0^{\omega+\alpha}, \quad k_3 \sim \tau_0^{\omega+\alpha-1}.$$

Here the value of the exponent calculated numerically is equal to  $\omega + \alpha$  with an accuracy to 2%, which could be expected. Hence, if  $\tau_0 \rightarrow 0$ , then the asymptotics (10) is “rebuilt” to that for the ideal bimaterial contact ( $\tau_0 = 0$ ). Moreover, the relations in (11) make it possible to calculate the constants  $C_0\mu_0, k_3$  in (10) for all values of  $\tau_0$  using the information concerning only one small value of  $\tau_0$ .

In Fig. 3, graphs of the stress intensity factor  $k_3$  (Fig. 3 a) and the ratio  $k/\gamma_0 = k/\omega_*$  (Fig. 3 b) are presented in a logarithmic scale as functions of  $\tau_0$  for  $\alpha = 1.0$

and different values of the ratio  $\mu_1/\mu_0$ . One can easily see that if  $\tau_0 = \tau\mu_0 \rightarrow 0$ , then all constants approach those for the ideal contact conditions:  $k_3 \rightarrow k_3^{id}$ ,  $\gamma_0 = \omega_* \rightarrow \omega$ .

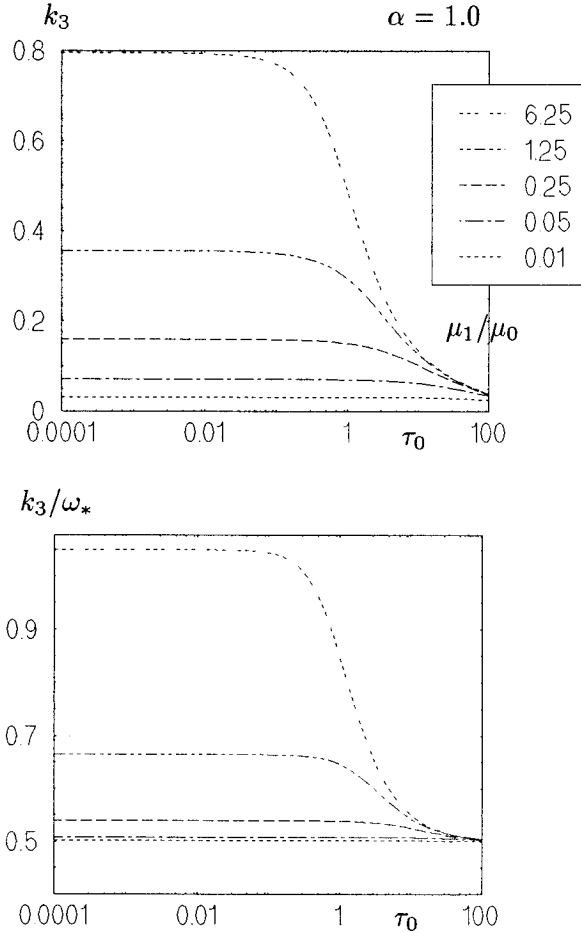


FIG. 3. Graphs of SIF  $k_3$  and the ratio  $k_3/\omega_*$  in the case  $\alpha = 1$  for different values of  $\tau_0$ .

Let us note that coefficient  $k_3/\gamma_0$  should be used in fracture mechanics analysis instead of the parameter  $k_3$  when the order of the stress singularity is not equal to  $-0.5$ . Actually, if we will consequently apply any of the critical tip opening fracture criteria [4, 6, 14], or the effective stress fracture criterion proposed by NOVOZHYLOV [11], which can be schematically written (without determining the stress-strain state) like this:

$$\Delta u(d, \theta) < v_*, \quad \frac{1}{d} \int_0^d \sigma(r, \theta) dr < \sigma_*, \quad \Rightarrow \quad \frac{kd^{\gamma_0}}{\gamma_0} < \text{const},$$



then the term  $k_3 d^{\gamma_0} / \gamma_0$  should be investigated. Here  $d$  is some additional parameter of the dimension of length which has a different sense for each fracture criterion. Note that the criterion [11] has been generalized by MROZ, SEWERYN [12, 13] for different fracture and failure processes.

Let us illustrate the fact that the value of the stress intensity factor can not completely determine the fracture process. Namely, from Fig. 1 and Fig. 3 a, it follows that  $\omega_* \rightarrow 0$ ,  $k_3 \rightarrow 0$ , when  $\mu_1 / \mu_0 \rightarrow 0$ . It means that the generalized SIF  $k_3$  tends to zero when the crack terminates at very soft material, and, consequently, one could conclude that the crack should not propagate. However, such the result is evidently false. Note in this connection that the exponent of stress singularity  $\omega_* - 1$  tends to  $-1$  at this time! On the other hand, from Fig. 3 b we can find that the value of  $k_3 / \omega_*$  does not tend to zero, and  $k_3 / \omega_* \rightarrow 0.5$  only.

Now we present the numerical results when parameter  $\alpha$  is greater than  $2 - \omega$ . In this case, the stress singularity exponent does not depend on all remaining parameters and is equal to  $\omega - 1$ . Hence, we can compare the respective unique value of  $k_3$  from (10) with the coefficient  $k_3^{\text{id}}$  corresponding to the ideal contact condition ( $\tau_0 = 0$ ).

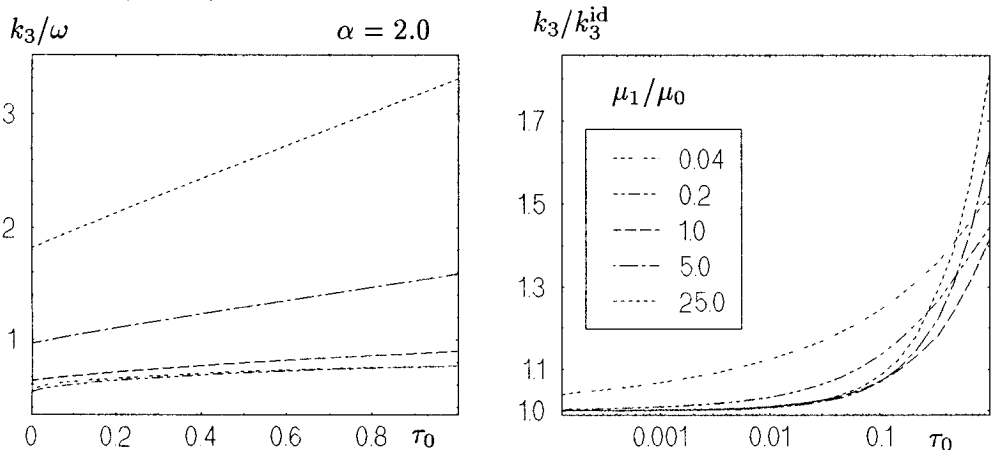


FIG. 4. Influence of the parameter  $\tau_0 = \mu_0 \tau$  on the SIF in the case  $\alpha = 2.0$ . Here  $k_3^{\text{id}}$  is SIF for the ideal model.

In Fig. 4, graphs of the parameters  $k_3 / \omega$ ,  $k_3 / k_3^{\text{id}}$  are presented as functions of parameter  $\tau_0$  for different values of the shear moduli ratio  $\mu_1 / \mu_0$  and for  $\alpha = 2.0$ . Because all curves in Fig. 4 a are straight lines when  $\tau_0 > 0.05$ , there is a linear dependence of  $k_3$  on this parameter for such values of  $\tau_0$ :

$$k_3 \approx k_3^{\text{id}} + \text{const}(\mu_1 / \mu_0, \alpha) \tau_0.$$

Let us note that this approximate relation for  $k_3$  is transformed into an equality for all values of  $\tau_0$  with  $\alpha = 1 + \omega$  when the value of  $k_3$  is calculated in a closed form.

The next conclusion that can be drawn is that parameter  $\tau_0$  influences weakly the stress intensity factor when  $\tau_0 < 0.1$ . (The corresponding ratio  $k_3/k_3^{\text{id}}$  is less than 1.1) Moreover, as the ratio  $\mu_1/\mu_0$  increases, the interval of parameter  $\tau_0$  extends where the stress intensity factor  $k_3^{\text{id}}$  is acceptable instead of  $k_3$ . Nevertheless, outside the mentioned interval of  $\tau_0$ , the largest departures of  $k_3$  from  $k_3^{\text{id}}$  occur for the largest values of  $\mu_1/\mu_0$ .

Using the results presented above, we can also investigate the influence of the ratio  $\mu_1/\mu_0$  on all parameters determining the brittle fracture process. Besides, some additional numerical results for different values of  $\mu_1/\mu_0$  and  $\alpha$  are presented in [10].

Passing to the influence of parameter  $\alpha$ , we note that the stress singularity near the crack tip is presented in each of the materials only if  $\alpha > 0$ . But if  $\alpha = 0$ , logarithmic singularity arises only in a half-plane of the shear modulus  $\mu_1$ . This contradiction is eliminated by the fact that function  $\text{ctg } \gamma_0(\pi/2 + \theta)$  ( $\gamma_0 = 1 - \alpha$ ) in the formulae (10) for  $\alpha > 0$  tends to zero as  $\alpha \rightarrow 0$ .

It seems to be natural to expect that  $k_3$  will approach  $k_3^{\text{id}}$  as  $\alpha \rightarrow \infty$ . However, this is not true in our case. This sudden paradox can be easily explained. Namely, in the model under consideration, it has been assumed that condition (1)<sub>1</sub> is satisfied along the whole bimaterial contact. However, when  $r \rightarrow \infty$  and  $\alpha > 1$ , the relative thickness of the intermediate zone is not small, which is in contradiction to the necessary assumption of the thin shell approach. As a result, the displacement does not vanish at infinity in our modelling problem (see the value of  $C_\infty$  in (10)). To eliminate such an inconsistency, it is necessary to correct the interfacial condition (1)<sub>1</sub> in the following way:

$$[u] = f(r, \tau, \alpha)\sigma, \quad f(r, \tau, \alpha) = \begin{cases} \tau r^\alpha, & 0 < r \leq a, \\ \tau, & a < r < \infty, \end{cases}$$

where  $a$  is some parameter. We shall not investigate the corresponding boundary value problem in the paper. Nevertheless, the asymptotic behaviour of stresses near the crack tip will coincide with that obtained above in (10).

For parameter  $\alpha \in (0.5, 2)$ , the coefficient  $k_3$  of the first asymptotic term cannot be used in fracture mechanics analysis only. The coefficients in the next singular terms should also be taken into account.

We can investigate the more general interfacial zone which is represented by two thin wedges connected with arbitrary interlayers considered above. Then the respective interfacial conditions are of the form:  $[u] = (r\tau + \tau_1 r^\alpha)\sigma$ ,  $[\sigma] = 0$ , instead of the relation (1), and the corresponding functional equation will be written as follows:

$$\mu_0 \tau_1 \tilde{\sigma}_0(s + \alpha - 1) + F_\tau(s) \tilde{\sigma}_0(s) = G(s).$$

Consequently, in this case we can obtain similar results as before with new parameters:  $\bar{\omega} = \omega_*(\tau_0)$  instead of  $\omega$ , and  $\bar{\omega}_* = \omega_*((\tau + \tau_1)\mu_0)$  instead of  $\omega_*(\tau_0)$ .

## 2. CRACK APPROACHING THE NONIDEAL INTERFACE

Now we investigate the Mode III problem for a semi-infinite crack approaching the layer from an infinite matrix. The crack is normal to the interface and the distance between the crack tip and the layer is  $h_1$ . The matrix is homogeneous and isotropic, but the layer is homogeneous and anisotropic with the main axes parallel and perpendicular to its boundaries. The corresponding elasticity moduli are  $\mu_x, \mu_y$ . The thickness of the layer is equal to  $h_2$ . Interfacial conditions are assumed to be nonideal with the parameters  $\alpha = 0, \tau > 0$ , e.g.  $[u_z] = \tau\sigma_{yz}, [\sigma_{yz}] = 0$ . Such situation corresponds to a thin adhesive intermediate layer that seems to be a natural occurrence. Finally, on the crack surfaces tractions are prescribed.

From the author's point of view, such a model is appropriate to investigate the main features of the interaction between the crack tip and two nearest nonideal interfaces of a composite.

Further on we will use the following normalized parameters:  $h_* = h_1/h_2, \tau_* = \tau\mu_0/h_2, \mu_* = \mu_1/\mu_0, \mu_l = \sqrt{\mu_x\mu_y}, a_l = \sqrt{\mu_x/\mu_y}$ .

The method of solution of a similar problem is developed in [8]. The Fourier and the Mellin transforms are applied to respective (layered and wedged) parts of the domain, and are fitted together along the common (interfacial) boundaries. Finally, the problem is reduced to a singular integral equation with fixed point singularities. We do not present here the accurate form of the equation (it has been derived in [7]), but show some numerical results only.

### 2.1. Numerical results

The stress singularity near the crack tip is always equal to 0.5. Hence, we can investigate only the value of SIF. As ATKINSON has proved in [1, 2], the asymptotic formula for SIF is of the form:

$$(12) \quad K = -\frac{D}{h^{1/2} \ln h} \left( 1 + O\left(\frac{1}{\ln h}\right) \right), \quad h \rightarrow 0,$$

when the crack tip is at a small distance  $h$  from the free boundary, or

$$(13) \quad K = Eh^{1/2-\omega} + O(h^{1/2-\omega_2}), \quad h \rightarrow 0,$$

when the crack tip is at a small distance  $h$  from the ideal interface. Here,  $\omega_2$  is the second zero of the function  $F(s)$  defined in (6), and  $D, E$  are some constants.

Let us compare the values of SIF obtained numerically by solving the mentioned singular integral equation, with those given by Eqs. (12) and (13).

In Fig. 5, the graphs of a normalized SIF  $k_3^*(h_*) = k_3(h_*)/k_3(\infty)$  are presented in a logarithmic scale as functions of the normalized distance  $h_*$  between the crack tip and the nearest interface of the isotropic layer ( $a_l = 1 \Leftrightarrow \mu_x = \mu_y$ ), for different values of parameter  $\tau_*$ .

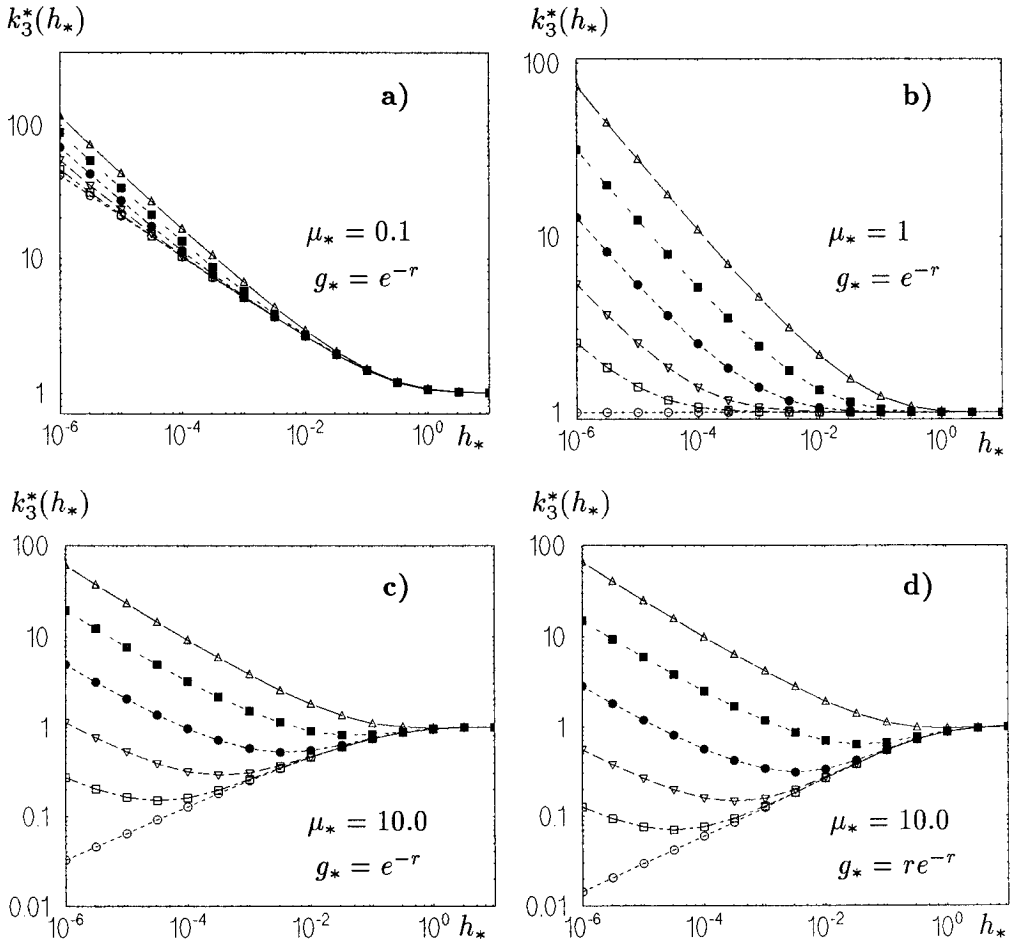


FIG. 5. Influence of normalized distance  $h_* = h_1/h_2$  between the crack tip and the nearest interface on normalized SIF  $k_3^*(h_*) = k_3(h_*)/k_3(\infty)$ , for different values of the ratio  $\mu_* = \mu_1/\mu_0$ , and the interaction parameter  $\tau_* = \mu_0\tau/h_2$ :  
 $\triangle$ --- $\triangle$  - 1.0,  $\blacksquare$ --- $\blacksquare$  - 0.1,  $\bullet$ --- $\bullet$  -  $10^{-2}$ ,  $\nabla$ --- $\nabla$  -  $10^{-3}$ ,  $\square$ --- $\square$  -  $10^{-4}$ ,  $\circ$ --- $\circ$  - 0.0.

Here  $k_3(\infty)$  is SIF for the semi-infinite crack in the homogeneous infinite plane under similar loading. In Fig. 5 a the layer is “soft” ( $\mu_* = \mu_1/\mu_0 = 0.1$ ); in Figs. 5 c and 5 d the layer is “stiff” ( $\mu_* = 10.0$ ); but in Fig. 5 b the shear moduli

of the layer and the matrix are similar ( $\mu_* = 1.0$ ). Besides, in Figs. 5 a, 5 b and 5 c the loading  $g_*(r) = e^{-r}$  is prescribed, but in Fig. 5 d,  $g_*(r) = re^{-r}$ .

As one can see, for different values of the ratio  $\mu_1/\mu_0$  the graphs for the ideal interfacial conditions ( $\tau_* = 0$ ) have linear portions for small values of  $h_*$  corresponding to the formula (13).

All curves for the nonideal contact have three specific portions. Firstly, the crack does not "feel" the bimaterial interface (horizontal lines). Secondly, the crack accepts the bimaterial as the ideal one. The curves for ideal and nonideal contacts coincide. The corresponding portions depend essentially on the values of the interacting parameter  $\tau_*$ . And, finally, when  $h_*$  is less than a certain value of  $h_*(\tau_*)$ , the crack "feels" the bimaterial interface as a free boundary. In this case, all curves are parallel, because the term  $\ln|\ln r|$  is smaller than the term  $\ln D - 0.5 \ln r$  (see (12)) when  $10^{-6} < r < 10^{-2}$ .

Further we investigate the influence of the distance between the crack tip and the nearest bimaterial interface  $h_*$  on the distribution of the traction along the interface.

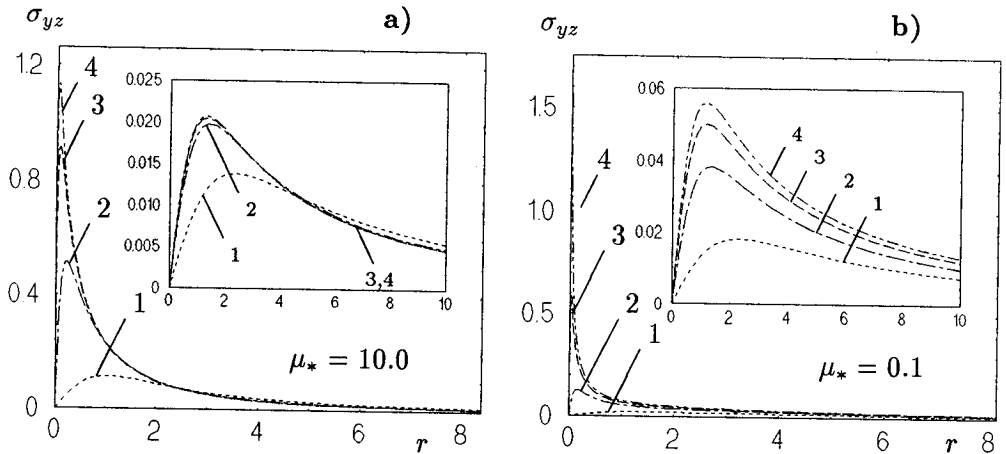


FIG. 6. Tractions along both interfaces for different normalized distance  $h_* = h_1/h_2$ :  
 1 - 1.0, 2 -  $10^{-1}$ , 3 -  $10^{-2}$ , 4 -  $10^{-3}$ .

In Fig. 6, the graphs of tractions  $\sigma_{yz}$  along the nonideal boundaries of the layer are presented. Here the figures of the usual size correspond to the nearest nonideal interface, and the smaller ones correspond to the next layer boundary. As before, the layer is assumed to be isotropic. Two different values of the ratio  $\mu_1/\mu_0 = 10.0, 0.1$  are considered in Fig. 6 a and Fig. 6 b, respectively. Finally, the loading  $g_* = e^{-r}$  is prescribed along the crack surfaces, and the value of the parameter  $\tau_*$  is  $\tau_* = 0.1$ . Let us note that, even though there is a significant stress concentration for small values of the distance  $h_*$ , the traction is equal to zero on the crack line ahead.

In Fig. 7, the graphs of tractions  $\sigma_{yz}$  along the nonideal boundaries of the layer are presented as functions of parameter  $\tau_*$  for fixed distance  $h_* = 0.01$  between the crack tip and the nearest interface. As before, the smaller figures correspond to the next layer boundary. The layer is assumed to be isotropic. Two different values of ratio  $\mu_1/\mu_0 = 10.0, 0.1$  are considered in Fig. 7a and Fig. 7b, respectively; and the loading  $g_* = e^{-r}$  is prescribed along the crack surfaces. What is important to note is that the tractions along the next nonideal contact are practically independent of the values of the parameter  $\tau_*$ . As it could be expected, the greatest concentrations of stresses correspond to the smallest values of the parameter  $\tau_*$ .

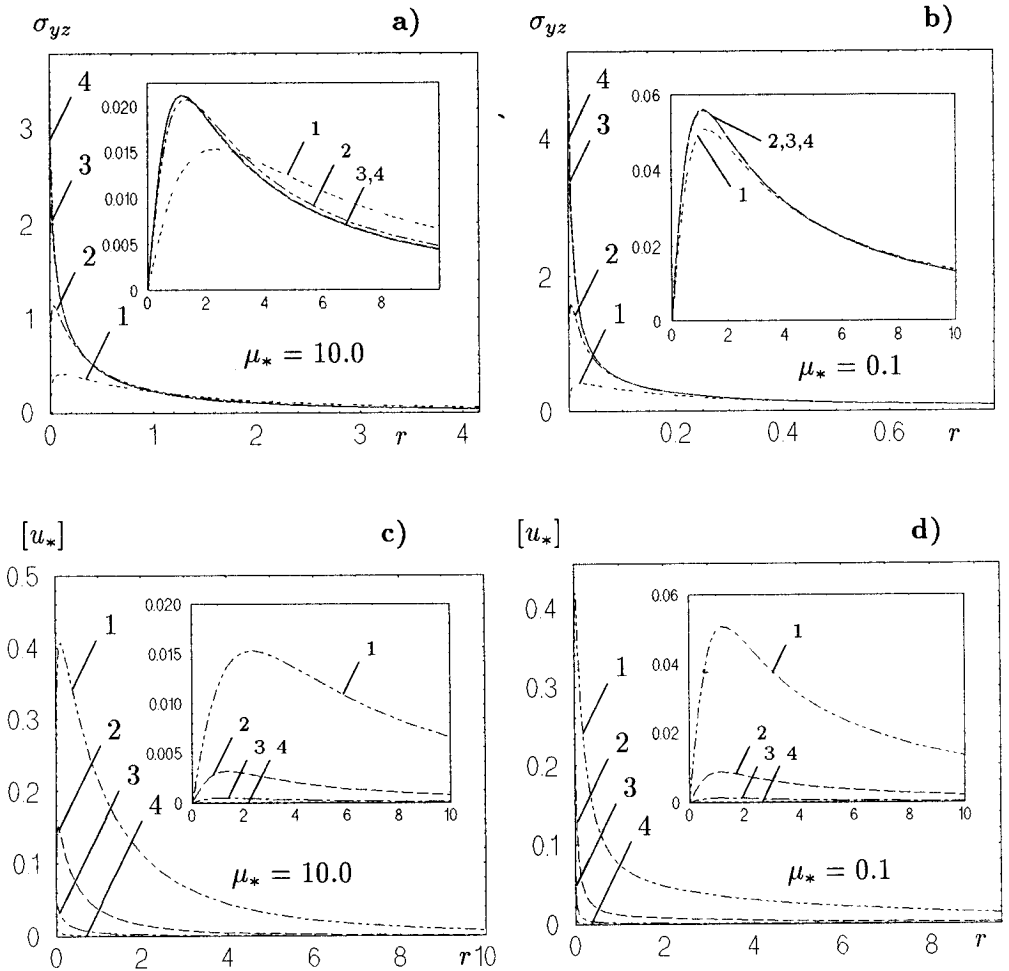


FIG. 7. Tractions  $\sigma_{yz}$  and normalized displacement discontinuity  $[u_*]$  along both interfaces for  $h_* = 0.01$  for different values of the interaction parameter  $\tau_*$ : 1 - 1.0, 2 -  $10^{-1}$ , 3 -  $10^{-2}$ , 4 -  $10^{-3}$ .

Now we investigate the influence of parameter  $\tau_*$  on the normalized values of the displacement discontinuity  $[u_*] = \mu_0[u_z]/h_2$  along the nonideal interfaces. The corresponding graphs are represented in Fig. 7 c, 7 d, where all parameters are similar to those in Fig. 7 a, 7 b. As one can see, the greatest values of parameter  $\tau_*$  correspond to the greatest values of the displacement discontinuity. This fact may explain the growth of an interfacial crack along the nonideal interface for such values of parameter  $\tau_*$ .

Basing on these and some additional numerical results presented in [7, 9, 10], the following main conclusions can be drawn.

### 3. CONCLUSIONS

When the FEM is used, the following circumstances should be taken into account to construct the necessary special elements and to determine the zones where such elements could be applied.

- Stress singularity near the crack tip terminating at the nonideal bimaterial interface ( $[\sigma] = 0$ ,  $[u] = \tau r^\alpha \sigma$ ) depends qualitatively on parameter  $\alpha$ , and is equal to the value  $\omega - 1$  corresponding to the ideal contact only if  $\alpha > 1$ .

- In general, the number of singular terms of asymptotic expansion of stress near the crack tip increases when  $\alpha \in (0.5, 1 + \omega)$ , and tends to infinity as  $\alpha \rightarrow 1$ . This fact is an additional argument that not only the main term of stress asymptotic expansion but all nonvanishing terms should also be taken into account in fracture mechanics analysis.

- If  $\alpha = 0$ , logarithmic stress singularity appears in front of the crack tip.

- When  $\tau_0 = \tau \mu_0 \ll 1$  (in most cases even if  $\tau_0 \leq 0.1$ ), asymptotic solution is rebuilt to the solution corresponding to the ideal contact at the distance  $r \sim \tau_0$  for an arbitrary value of  $\alpha$ .

- Crack interacts with the nonideal contact ( $\alpha = 0$ ) at the distances between the crack tip and the nearest bimaterial interface greater than a certain value  $h(\tau_*)$ , ( $\tau_* = \tau \mu_0 / h_2$ ) as it interacts with the ideal contact. But, already for distances  $h_* \leq h(\tau_*)$ , the crack “feels” the nonideal interface as a free boundary. This could explain the hunting crack phenomenon, and the corresponding initiation of an interfacial crack.

- The greatest influence of the interaction parameter  $\tau_*$  appears when the shear modulus of the matrix is less than the mean value of modulus  $\mu_l = \sqrt{\mu_x \mu_y}$  of the anisotropic layer (when the layer is rigid).

- Tractions on the opposite side of the layer (along the next nonideal interface) are practically independent of  $\tau_*$ . Hence, the parameter  $\tau_*$  can be taken into account for the nearest nonideal interface only.

- Anisotropy of the layer influences essentially the results when the layer is rigid ( $\mu_l > 10\mu_0$ ).
- Distribution of the tractions along the crack surfaces leading to the same resultant force has the greatest influence on the SIF when the contact is ideal.

## REFERENCES

1. C. ATKINSON, *On the stress intensity factor associated with cracks interacting with an interface between two elastic media*, Int. J. Engng. Sci., **13**, 489–504, 1975.
2. C. ATKINSON and H. JAVAHERIAN, *Evaluation of stress intensity factors associated with bimaterial cracks*, J. Inst. Maths Applies, **26**, 235–258, 1980.
3. G.P. CHEREPANOV, *Mechanics of brittle fracture*, Mc Graw-Hill, New York 1979.
4. D.S. DUGDALE, *Yielding of steel sheets containing slits*, J. Mech. Phys. Solids, **37**, 197–208, 1960.
5. *Interlaminar response of composite materials*, N.J. PAGANO [Ed.], Composite Materials Series, **5**, Elsevier, Amsterdam-Oxford-New York-Tokyo 1989.
6. M.YA. LEONOV and V.V. PANASYUK, *Evolution of small cracks in solid bodies* [in Ukrainian], Appl. Mech., **5**, 391–401, 1959.
7. G.S. MISHURIS, *On the interaction of a turnpike crack with nonideal bimaterial interfaces in a layered composite* [in Russian, translated into English], Mechanics of Composite Materials, **30**, 6, 591–610, 1994.
8. G.S. MISHURIS and Z.S. OLESIAK, *On boundary problems in fracture of elastic composites*, Euro. J. Appl. Math., **6**, 591–610, 1995.
9. G.S. MISHURIS, *Influence of interfacial models on a stress field near a crack terminating at a bimaterial interface*, Int. J. Solids Structures, **34**, 1, 31–46, 1997.
10. G.S. MISHURIS, *Stress singularity as a function of a model of nonideal bimaterial interface (Mode III)*, Int. J. Solids Structures [in press].
11. V.V. NOVOZHYLOV, *On necessary and sufficient criterion on brittle fracture*, Prikl. Mat. Mech. (PMM), **33**, 212–216, 1969.
12. A. SEWERYN, *Brittle fracture criterion for structures with sharp notches*, Engng. Fract. Mech., **47**, 673–681, 1994.
13. A. SEWERYN and Z. MRÓZ, *A non-local stress failure conditions for structural elements under multiaxial loading*, Engng. Fract. Mech., **51**, 955–973, 1995.
14. A.A. WELLS, *Critical tip opening displacement as fracture criterion*, [in:] Proc. Crack Propagation Symp. Granfield, **1**, 210–221, 1961.

DEPARTMENT OF MATHEMATICS,  
TECHNICAL UNIVERSITY OF RZESZÓW

W. Pola 2, 35-959, Rzeszów, Poland  
e-mail: miszuris@prz.rzeszow.pl

Received October 21, 1996.

---